New Journal of Physics
The open access journal at the forefront of physics
Deutsche Physikalische Gesellschaft DPG | IOP Institute of Physics

Quantum size effects in chemicurrent measurements during low-temperature oxidation of Mg(0001) epilayers

Ulrich Hagemann and Hermann Nienhaus

Faculty of Physics, University of Duisburg-Essen and Center of Nanointegration Duisburg-Essen (CENIDE), Lotharstr. 1, D-47048 Duisburg, Germany
E-mail: hermann.nienhaus@uni-due.de

Received 14 July 2014, revised 17 September 2014
Accepted for publication 3 October 2014
Published 14 November 2014

New Journal of Physics **16** (2014) 113035

doi:10.1088/1367-2630/16/11/113035

Abstract

The reactivity of Mg epilayers on Si(111)-7 × 7 towards molecular oxygen is investigated as a function of the metal film thickness in the range between 7 and 45 monolayers. Quantum well and surface states are characterized with ultraviolet photoelectron spectroscopy demonstrating the epitaxial and single-crystalline structure of the Mg films. The oxidation rate is monitored during the reaction by measuring chemicurrents at 110 K in the Mg/p-Si(111) Schottky diodes due to the non-adiabatic character of at least one step in the reaction chain. For film thicknesses around 9 and 13 monolayers the chemicurrent transients demonstrate that the reaction rate is strongly enhanced by a factor of more than two. With Mg 2p core level spectroscopy, a similar enhancement can be found for the total oxygen uptake for long exposures indicating that the chemicurrent increase measures solely a quantum size effect on the reactivity and no device-related effects. The enhanced reactivity can be explained by the increased first charge transfer into the affinity level of the approaching molecule when a quantum well state appears at the Fermi level and increases the density of electronic states. A linear relationship between the photoelectron intensity at the Fermi level and the maximum chemicurrent is clearly observed. On the other hand, the surface work function and the Schottky barrier height exhibit almost no correlation with the enhanced reactivity.

Keywords: quantum size effect, oxidation, magnesium, epilayer, non-adiabatic, chemicurrent, quantum well state

1. Introduction

Tuning the chemical activity of a surface has been an aspiration for a long time as it allows one to control the decisive steps in important processes like heterogeneous catalysis [1], gas sensing [2] or corrosion and passivation chemistry [3]. Different tools have emerged from the huge effort put into this issue. Today, the reactivity can be enhanced by extrinsic means like photon irradiation in photochemistry [4] or change of the electrochemical potential in electrochemistry [5] as well as by preparation of intrinsic material properties changing the structure and reducing the size [6–10]. The latter has been impressively demonstrated by making the noble metal gold catalytically active by reducing the particle size [9–11]. The wide field of nanocatalysis and chemistry at nanostructures has given numerous other examples [12].

The physics behind the size-dependent surface chemistry at metal particles is based on the variation of the surface electronic structure. This may happen locally due to the usually large number of low-coordinated metal atoms at the nanoparticle surface [6, 13, 14] or by the global effect of spatial confinement of the electrons usually referred as quantum size effects (QSEs) [11, 15–21]. Which of the two contributions dominates the reactivity depends on the system and is often difficult to decide as the chemistry at nanoparticles is typically studied at large inhomogeneous ensembles with at least billions of particles. To distinguish between local effects and QSE, gas-surface reactions at epitaxial thin metal films may be studied which form quantum wells and confine the electronic states perpendicular to the surface. The films may extend laterally on macroscopic dimensions and show an almost defect-free crystalline structure. Such epilayers exhibit a small periodic variation of surface physical properties with film thickness like the photoelectron intensity at the Fermi level E_F for $\vec{k}_{||} = 0$ and a fixed k_z, the decay length of surface states into vacuum or the work function [20, 21, 23–28]. The photoelectron intensity is often taken as a measure for the total density of states (DOS) at E_F, although the yield corresponds to a certain $\vec{k}$ vector and is further determined by the final state density. In addition, the k_z component depends on the photon energy and the unknown surface potential [22]. However, in most cases the qualitative variation of the DOS is of interest instead of its absolute value. Then, it is reasonable to assume that measured photoelectron yield and DOS exhibit equal variations with metal film thickness. Yet, the DOS and the decay length are quantities which determine the gas-surface reactivity in particular when charges are transferred between the metal and the approaching gas particle in the course of the reaction.

The oxidation of non-noble metal surfaces by interaction with thermal O_2 molecules is a multi-electron transfer process since in most cases oxygen is dissociated and the atoms have eventually the oxidation state of minus two. It is an excellent model reaction for QSEs in the reactivity and has been studied for Mg [18, 20], Al [19] and Pb epilayers [17, 21] on semiconductor and metal surfaces. In the case of Mg surfaces, quantum well states (QWSs) can be well observed and an enhanced oxygen uptake is recorded with x-ray photoelectron microscopy (XPEEM) for epilayer thicknesses of 7 monolayers (ML) [18, 19, 28]. In general, theory confirms the observation, however, it predicts a reactivity maximum for 9 ML [20]. The XPEEM measurements were performed by interrupting the exposure and *a posteriori* surface analysis which is a disadvantage due to potential contaminations and to residual oxygen doses

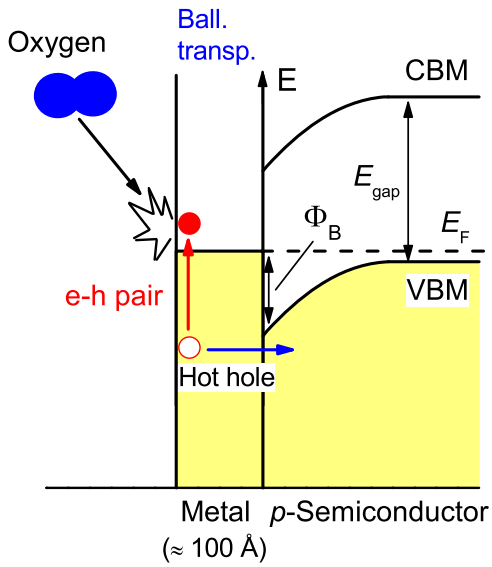

Figure 1. Principle of chemicurrent measurements with p-type thin metal film Schottky diodes: the non-adiabatic surface reaction generates electron–hole pairs; the hot hole travels ballistically to the interface and causes a reverse current in the device if the kinetic energy is larger than the barrier height Φ_B. VBM: valence band maximum; CBM: conduction band minimum.

during interruption. Fortunately, the oxidation of metal surfaces includes reaction steps, e.g., the dissociation, which may occur non-adiabatically on a very short time scale. As a consequence, the reaction excites electron–hole (e–h) pairs in the metal leading to external and internal exoelectron emission [29–32]. The chemicurrent method allows the detection of chemically induced hot charge carriers [33–35]. It monitors the reaction and measures the reaction rate during the interaction without the need of interrupting the experiment. This has been successfully demonstrated for the oxidation of polycrystalline Mg surfaces using Mg/p-Si Schottky diodes [30].

Chemicurrents are detected in thin-film electronic devices. The principle is shown in figure 1 for a p-type doped Schottky diode. The reaction excites an e–h pair due to a non-adiabatic interaction, e.g., a charge transfer. The hot hole can travel ballistically from the surface to the interface and may surmount the Schottky barrier if the kinetic energy is larger than the barrier height Φ_B. Since Φ_B is typically below 1 eV and therefore much smaller than any work function the internal detection is orders of magnitude more sensitive than exoelectron emission measurements into vacuum. In the present study, we fabricate Mg-*p*-Si(111) Schottky diodes with epitaxial and crystalline Mg films. The evolution of QWSs are clearly resolved with photoemission demonstrating the excellent metal film and surface quality. Additionally, the metal-semiconductor interface is of high quality as the devices exhibit excellent rectifying properties. Chemicurrent measurements are performed during thermal oxygen exposure showing directly the reactivity of the surface varying with epilayer thickness.

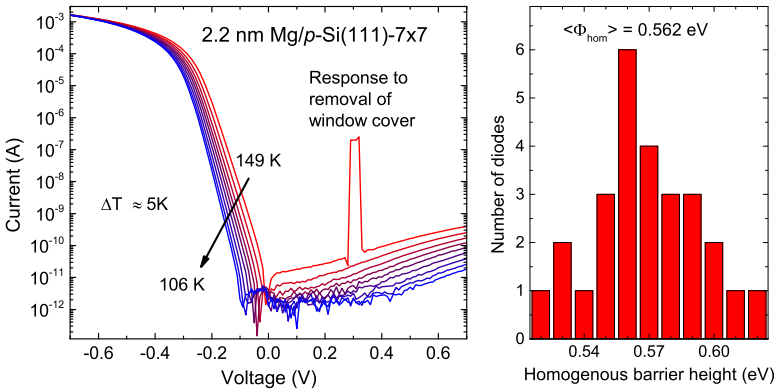

Figure 2. Left panel: current–voltage characteristics of a Mg/p-Si(111) Schottky diode with a metal film thickness of 2.2 nm for various temperatures. The increase in the reverse direction is due to a photocurrent. Right panel: distribution of homogeneous Schottky barrier heights of Mg/p-Si(111) diodes of various film thickness.

2. Experimental methods

The experiments are performed under ultrahigh vacuum conditions (UHV, $p_0 \leqslant 10^{-8}$ Pa). Thin Mg film Schottky diodes are fabricated on p-type Si(111) wafer pieces with a specific resistivity of 7.5 Ωcm. To achieve the 7 × 7 reconstruction of the substrates, the Si(111) surfaces are hydrogen passivated by etching in buffered hydrofluoric acid for three minutes, then being immediately transferred into the UHV chamber and annealed first to 600° and then repeatedly to 730° for five seconds. The surface reconstruction is controlled by low-energy electron diffraction (LEED). Magnesium epilayers are prepared by thermal evaporation at substrate temperatures below 120 K and evaporation rates below 1 ML min^{-1} using a shadow mask. The absolute film thickness is determined by measuring the deposition rate using a quartz microbalance. Values range between 2 and 12 nm, or 7 to 45 ML where one ML corresponds to 0.27 nm. Relative changes of the film thickness can be precisely determined by the energetic position of the quantum well levels. No oxygen or carbon contaminations can be found in any of the various preparation steps using x-ray photoelectron spectroscopy (XPS). Oxygen contaminations of less than one percent of a ML can be detected by ultraviolet photoemission (UPS) using HeI light (21.2 eV) from a gas discharge lamp (SPECS UVS10). UPS is known to be much more sensitive for oxygen detection than XPS. After deposition, the samples are annealed to room temperature (RT) to improve the film quality.

In situ current–voltage (*I*/*V*) characteristics are recorded in the low-temperature range between 100 and 170 K avoiding any irradiation of visible light. The diode front contact is formed after approaching a small Au ball towards the surface. The diode area is fixed to 72 mm^2. Typical *I*/*V* curves in a semi-logarithmic plot are shown in the left panel of figure 2 for a 2.2 nm Mg/p-Si(111)-7 × 7 Schottky diode during cooling down. The diodes are very photosensitive. The photoresponse when light is allowed into the chamber is shown in the reverse current which increases by more than three orders of magnitude. At temperatures below 120 K an open-circuit photovoltage of 0.1 V appears due to thermal radiation from the 300 K chamber walls. Applying thermionic emission theory [36] the effective Schottky barrier height Φ_B, the ideality factor n and the serial resistance can be extracted from the forward direction of the *I*/*V* curves [37]. The homogeneous barrier height which is relevant for chemicurrent

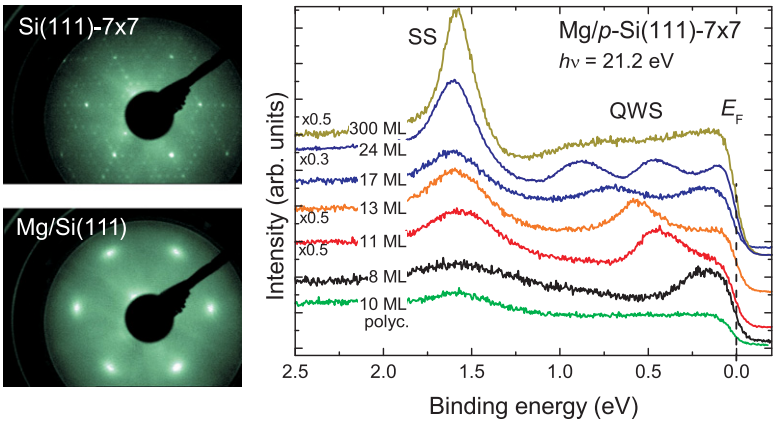

Figure 3. Left panel: LEED images of the Si(111)-7 × 7 surface after flashing the sample to 730 °C and of the Mg/Si(111)-7 × 7 surface after low temperature deposition of 6 nm Mg and soft annealing. The electron energy is set to 85 eV. Right panel: UP spectra of Mg films of different film thickness. SS: surface state; QWS: quantum well states.

measurements is determined by extrapolation of $\Phi_B(n)$ at the various temperatures to $n = 1.01$ [37]. The distribution of homogeneous barrier heights of numerous diodes is shown in the right panel of figure 2. An average value of (0.56 ± 0.02) eV is found. No correlation can be found between Mg film thickness and barrier height.

UPS spectra are recorded at RT using unpolarized and non-monochromated HeI light. The angle between the incident light and the entrance lens of the analyzer is fixed at 45°. The photoelectrons are analysed in normal emission by a hemispherical electron spectrometer (SPECS Phoibos100) with an acceptance angle set to ±3°. The surface work function is determined by the width of the UP spectra.

Chemicurrents are detected as reserve currents in the diodes during exposing the devices to molecular oxygen at low temperatures of typically 110 K. The chamber is backfilled with oxygen gas up to a pressure of 10^{-6} Pa by opening a leak precision valve corresponding to a flux of $q = 2.7 \times 10^{12}$ molecules $(\mathrm{cm}^{-2}\,\mathrm{s}^{-1})$. The backfilling pressure is controlled continuously using a cold cathode ionisation gauge line-off-sight from the sample surface. Thus, no measurable activation of the oxygen or the surface occurs during exposure.

3. Experimental results

3.1. Quantum well states

The quality of the Mg epilayers can be demonstrated by LEED and UPS. The left panel of figure 3 displays two LEED images with an electron energy of 85 eV taken from one sample after Mg deposition and annealing. The Si(111)-7 × 7 reconstruction is observed at sample sites behind the shadow mask where the pristine Si surface is preserved. The diffraction image of the 6 nm Mg film reveals a single domain Mg(0001) orientation. The azimuthal broadening of the LEED spots is caused by a rotational disorder of ±2°. The right panel of figure 3 shows UPS spectra of Mg epilayers ranging between 8 and 300 ML. The strong structure SS at a binding energy of 1.6 eV is attributed to the well-known Mg surface state [28, 38]. The features between

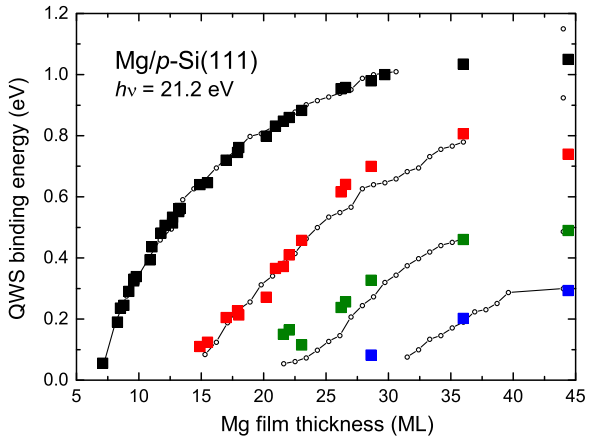

Figure 4. Energetic shift of the QWSs for samples with different film thickness. The connected small symbols represent data from literature [28].

the Fermi level and SS are due to Mg QWSs as they have been characterized in earlier studies [28]. They are not observed if the Mg film is polycrystalline or too thick as shown in the figure for the 10 and 300 ML film. The polycrystalline Mg film does not show a LEED image and has been fabricated by RT evaporation. The surface state is apparently less sensitive to structural disorder than the QWS.

The binding energies of the QWSs depend sensitively on the film thickness as summarized in figure 4. The diagram displays the position of the QWSs between SS and E_F as a function of the film thickness. The binding energy is measured relative to E_F. For films above 15, 21 and 27 ML, two, three or four QWSs can be resolved, respectively. The large symbols are results from the present study whereas the lines and small symbols represent reported energy positions [28]. The observed shifts agree very well with the literature data. As explained in detail elsewhere, the energetic position and the number of detectable QWSs is a consequence of spatial confinement of the electron waves including phase matching conditions at the interfaces [27, 28]. The present results give evidence for the well-defined layer thickness and crystalline structure of the large-area Mg epilayers on Si(111).

3.2. Chemicurrent response

When exposing the pristine Mg/p-Si(111) diodes to molecular oxygen a reverse current is detected due to the non-adiabatic dissipation of chemical energy. A typical chemicurrent response curve is shown in figure 5 recorded from a 32 ML Mg/Si diode together with the pressure variation which represents the accomodation of the system into equilibrium after opening the leakage valve at $t = 0$. The current starts at a low value, increases to a maximum and levels off for larger exposures. This behavior has been discussed in detail earlier and represents the chemical kinetics of the reaction [30] described by a nucleation-and-growth mechanism [39]. Oxygen molecules impinging on the Mg surface are dissociated at certain reaction sites which are identified with the edges of the growing oxide islands. Hence, the pristine Mg surface is rather inert to oxidation which initially starts at existing defect sites or contaminations leading to the non-zero current at $t = 0$. A part of the approaching molecules experiences a charge transfer to O_2^- and is physisorbed in a mobile precursor state on the surface. They are dissociated when they arrive at an oxide edge. Consequently, the

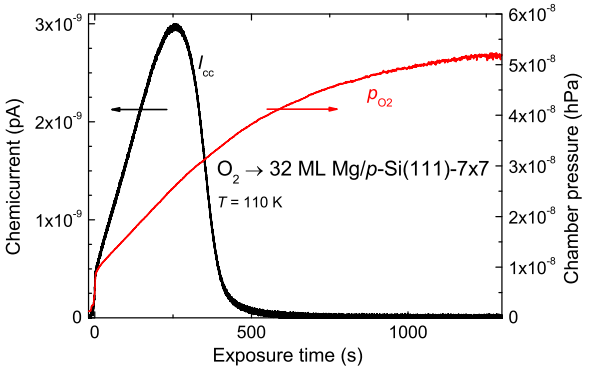

Figure 5. Chemicurrent curve and O_2 backfilling pressure as recorded. The typical shape of the chemicurrent transient represents the reaction kinetics according to a nucleation-and-growth mechanism.

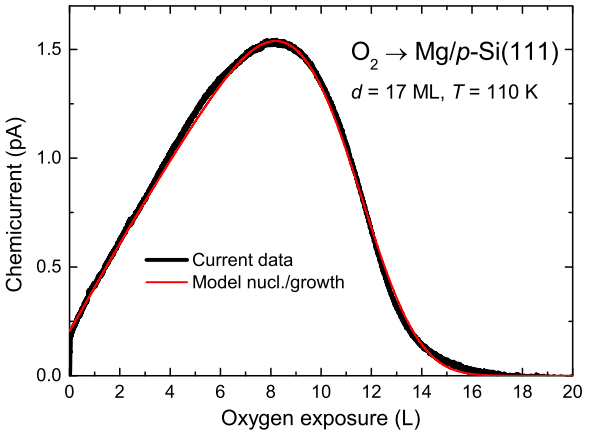

Figure 6. Chemicurrent as a function of the oxygen expsoure. The red line is calculated based on a modified nucleation and growth model.

chemicurrent which measures the reaction rate [33] increases with growing oxide islands until they begin to coalesce. Then, a rapid decrease of the island edge length and the corresponding reaction site density occurs as observed in the strong reduction of the chemicurrent. The kinetics of the oxidation of polycrystalline Mg surfaces can be well described within a simple nucleation-and-growth model [30] yielding $I_{cc}(t) \propto 2\,KN_0q^2t\,\exp\left[-KN_0q^2t^2\right]$ with q as the molecular flux and KN_0 as a model parameter proportional to the surface diffusion constant. The maximum of the chemicurrent curve occurs typically at a coverage of 0.4 ML.

In the present case, the recorded chemicurrents can be fitted by a modified nucleation-and-growth model assuming two different diffusion constants for the metal and oxide surfaces, respectively. In figure 6 the chemicurrent transient from a 17 ML Mg/p-Si(111) diode is plotted now as a function of the exposure. The solid line is calculated from the model with a varying KN_0 parameter between $6 \times 10^{-31}\,\mathrm{cm}^{-4}$ for the metallic Mg surface and $6 \times 10^{-32}\,\mathrm{cm}^{-4}$ for MgO indicating a much reduced diffusivity of O_2^- molecules on the oxide islands than on the metallic surface. Further details of the kinetics will be published in a separate article.

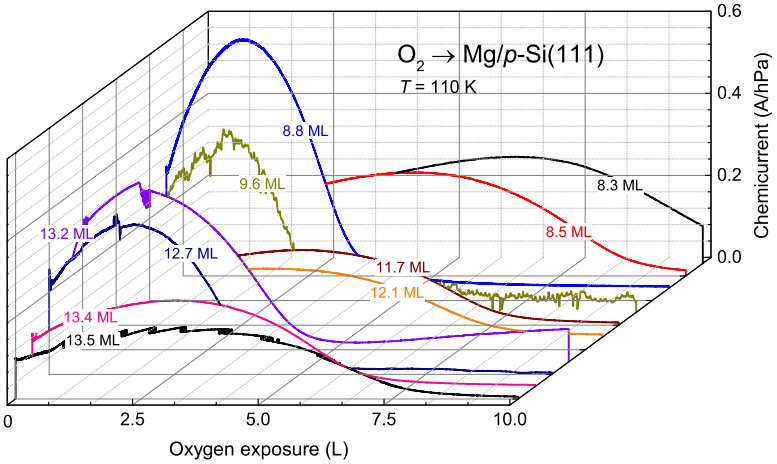

Figure 7. Chemicurrent traces for different Mg film thicknesses. Due to an increase of the reaction rate the current trace exhibits a larger maximum and is compressed for thicknesses of 9 and 13 ML.

3.3. Quantum size effects

Chemicurrent measurements are performed at Mg epilayers in the thickness range between 7 and 45 ML. The pressure changes during the exposures are accurately monitored allowing plots with a pressure-independent exposure axis as shown in figure 6. To compare the chemicurrent data the current values are divided by the actual pressure value yielding an efficiency of detected charge per molecule flux measured in A/hPa. Figure 7 shows a collection of chemicurrent recordings for various Mg/p-Si(111) diodes. There are two narrow thickness intervals around 9 as well as 13 ML where the efficiency is significantly enhanced and the curve is narrower than for traces outside the specific intervals. Indeed, the different curves in figure 7 can be transferred into a standard form by applying a scaling factor of stretching the exposure and of compressing the efficiency axis. This finding indicates that the surface reaction rate is enhanced for the respective thicknesses. Any effects due to device changes can be excluded. If the device had an increased detection efficiency for certain Mg thicknesses the chemicurrent would be larger as well, however, the curve would not be compressed on the exposure axis. We take the maximum value of the chemicurrent I_{max} as an indicator for the reactivity of the Mg surface since the exposure at maximum corresponds to a fixed coverage of approximately 0.4 ML. The initial chemicurrent at $t = 0$ is not appropriate to study the reactivity. In the nucleation and growth mode it is expected to be almost zero. However, an initial chemicurrent is indeed observed due to the non-vanishing nucleation site density on the unexposed surface. The initial number of nucleation sites is determined by structural defects, e.g., step sites, and fluctuates from sample to sample due to tolerances in the preparation procedure. Still, the density is sufficiently small that its variation cannot be observed in the photoelectron spectra of the SS and QWS. On the other hand, the maximum chemicurrent is determined by intrinsic properties of the Mg films like the layer thickness and is not affected by variations in the preparation. In figure 8 the circles represent the normalized chemicurrent at maximum as a function of the Mg film thickness showing the pronounced current maxima at 9 and 13 ML. As extracted from the figure, the chemicurrent and therefore the rate of oxidation is by a factor of two to three larger for the selected samples. The chemicurrent monitoring yields this result much more easily and

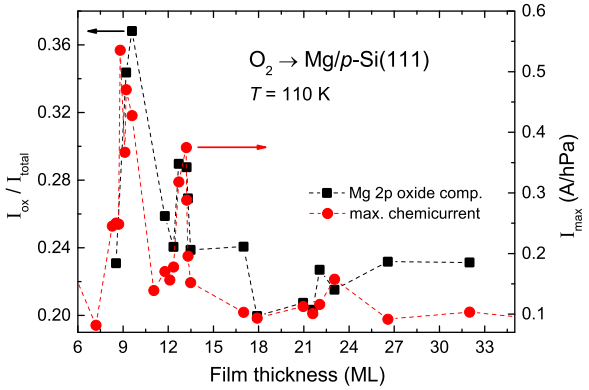

Figure 8. Oxide component of Mg 2p core level (black) and maximum chemicurrent (red) as a function of Mg film thickness.

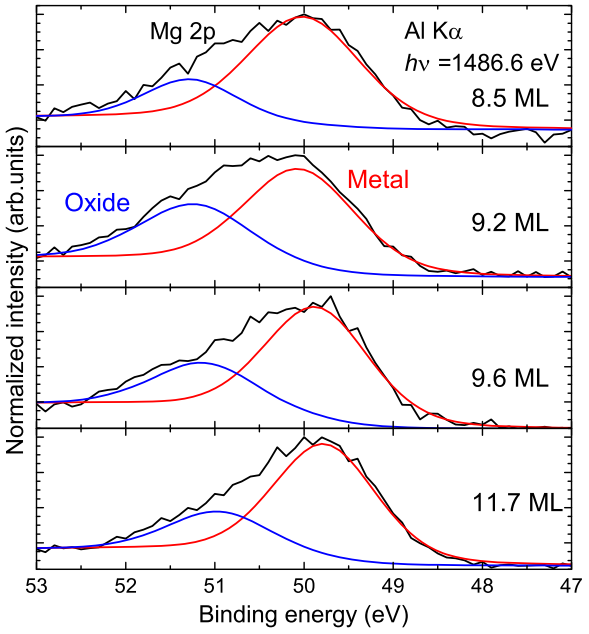

Figure 9. XPS measurements of Mg 2p core level fitted with two components, Mg oxide and Mg metal.

with a higher precision than XPEEM [18] which requires interrupting exposures and fitting procedures of the Mg 2p core level.

Yet, to compare chemicurrent results with chemical analysis we performed XPS to measure the total oxygen uptake with varying film thickness. The squares in figure 8 display the intensity of the oxide component in the Mg 2p core level. The spectra are taken after long oxygen exposures of typically 15 L. Respective Mg 2p core levels are shown in figure 9 for Mg films between 8.5 and 12 ML. The photoelectron lines are fitted with two components related to the metallic and the oxide species shifted by 1.2 eV. It is remarkable that the total oxygen uptake after large exposures follows a similar thickness dependence as the maximum chemicurrent (black squares in figure 8). While the chemicurrent measures the live reaction rate at a specific time the chemical analysis yields the *a posteriori* oxygen content of the surface.

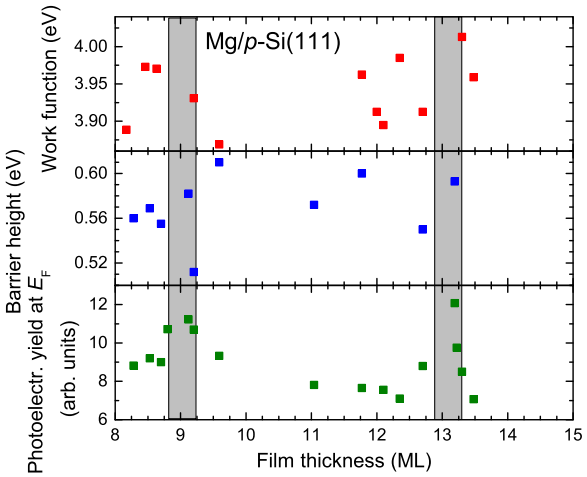

Figure 10. Work function, Schottky barrier height and photoelectron yield in normal direction at the Fermi level as a function of Mg film thickness. The yield is taken as a measure for the density of electronic states at E_F and exhibits enhanced values at the regions of interest. Interface and surface barriers show only statistical variations with film thickness.

Apparently, the more reactive the Mg films are the more they absorb oxygen in long exposure runs.

It has been reported earlier that an enhancement of the reactivity occurs for epilayers with an increased density of electronic states (DOS) at the Fermi level E_F [18]. Due to the shifting QWSs the photoelecton intensity at E_F is a periodic function of the film thickness. As pointed out in the Introduction, we neglect details in the photoemission process and take the photoelectron yield in normal emission as a measure for the DOS. We emphasize again that this is only possible, because we are interested in qualitative changes of the DOS with film thickness, i.e., whether the DOS is increased for certain thicknesses. The qualitative evidence does not depend on any k_z dependence in the photoemission process as the QWSs do not disperse with the perpendicular component of the wavevector. The present study gives a periodic variation of the photoelectron yield with metal film thickness as well. This is shown in the lowest panel of figure 10. The grey shaded areas highlight the thickness ranges where the enhanced chemicurrents are observed. Indeed, for Mg/p-Si(111) diodes with large chemicurrents and therefore high chemical reactivities the DOS is almost twice as large as for other diodes. The relation between DOS and reactivity will be discussed in the next section. The change of the Schottky barrier height and the surface work function with Mg film thickness is displayed in figure 10 as well. Both quantities are statistically distributed around the average value. The barrier height exhibits no significant correlation to any QSEs. For the work function a slight increase for certain epilayer thicknesses might be noticed as predicted by theory [24].

4. Discussion

4.1. Thickness dependence of chemicurrent

The chemicurrent is based on a ballistic transport of excited charge carriers through a metal film and is attenuated exponentially with film thickness, i.e., $I_{cc} \propto \exp[-d/\lambda]$ [33]. The mean free

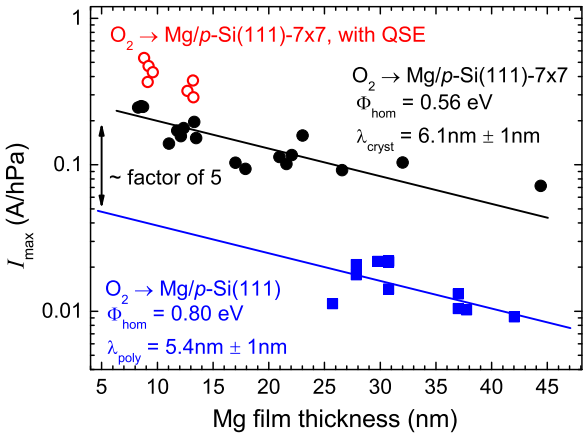

Figure 11. Attenuation of the maximum chemicurrent with Mg film thickness. Red open circles: diodes with enhanced values due to QSEs; black circles: diodes with Mg epilayers and no QSEs; blue squares: diodes with polycrystalline Mg films and lower barrier height from literature [30].

path λ is typically of the order of 10 nm as demonstrated in figure 11. The diagram shows the thickness dependence of the maximum chemicurrent during oxidation of Mg thin films on p-Si (111) substrates on a semi-logarithmic scale. The squares are data from polycrystalline Mg layers with a Schottky barrier height of 0.8 eV [30]. The circles are from the present study. If the exceptionally enhanced current values (open circles) are ignored the linear fit yields a mean free path of 6.1 nm which equals the value of 5.4 nm from the earlier data within the error margins. The factor of five between the chemicurrent strengths is due to the different barrier heights. The Schottky barrier of the epilayer diodes is much lower allowing more hot holes to contribute to the chemicurrent. The open circles in figure 11 demonstrate again the strong enhancement of the maximum chemicurrent by a factor of two to three due to QSEs. Evidently, the two groups of enhanced currents are attenuated with film thickness with the same λ-value as the other diodes. This is additional evidence that the chemicurrent enhancement originates from the surface reaction and cannot be explained with a transport effect.

4.2. QSE induced reactivity enhancement

The strong increase of the chemicurrent for certain epilayer thicknesses is related to the reactivity and not to any transport or barrier effects. The latter would not compress the chemicurrent curve along the exposure axis as it is observed. To understand why the epilayer thickness affects the chemistry we consider the subsequent steps of the reaction. The kinetics of the reaction has been described above to explain the chemicurrent transients. While approaching the surface the molecule experiences a first electron transfer from the surface as soon as the molecular affinity level is resonant with the Fermi level. Since this first charge transfer ($O_2 \rightarrow O_2^-$) occurs at relatively large distances from the topmost metal atoms it is often called *harpooning* [29, 40]. The charged molecule remains in the diffusive precursor state until it reaches a reactive site presumably the edge of a growing oxide island where further, non-adiabatic charge transfers [40], dissociation and oxidation occur. In particular, any changes of the surface electronic structure have a strong influence on the harpooning process and on the initial sticking coefficient into the physisorbed state. Hence, if the adsorption into the precursor

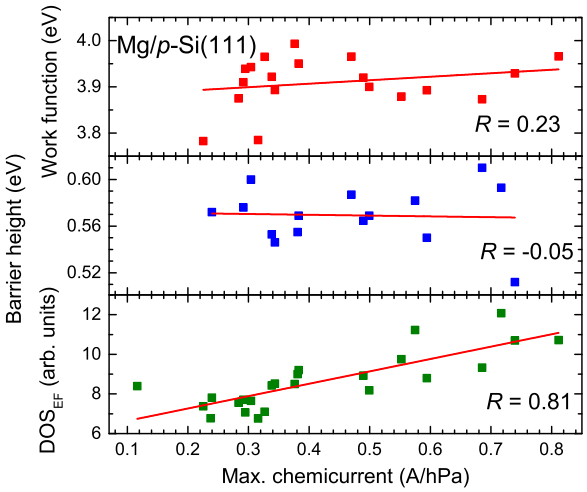

Figure 12. Correlation diagram between maximum chemicurrent and the quantities work function, Schottky barrier height and DOS. The Pearson coefficient R measures the linear relationship indicating the obvious correlation between DOS and chemicurrent strength.

state is *ceteris paribus* enhanced the reaction rate and consequently the chemicurrent would change as it is observed in figure 7. The chemicurrent is stronger and the saturation coverage is reached earlier.

The DOS close to the Fermi energy significantly varies with thickness due to the appearance and shift of the QWS. As shown above, both quantities, DOS at E_F and chemicurrent at maximum, are increased for thicknesses around 9 and 13 ML. This is again demonstrated in figure 12 where the work function, the Schottky barrier height and the DOS as measured by the photoelectron yield are plotted against the maximum chemicurrent for the variety of Mg/p-Si(111) diodes of different film thickness. The Pearson correlation coefficient R is calculated to analyse any linear relationship between the quantities. For $R = \pm 1$ there is a strong correlation whereas a vanishing R value denotes no linear correlation. DOS and current exhibit a clear linear relationship whereas the barrier height is independent and almost constant. The work function exhibits a slight correlation as it is expected. The work function is known to vary weakly with thickness for perfect epilayers [24]. The increase of the DOS at E_F influences directly the charge transfer rate into the affinity level of the molecule as the number of transferable electrons is larger and the electronic states at E_F decay farther into vacuum. The DOS of Mg epilayers has been calculated by Binggeli and Altarelli [20]. They found the largest DOS for 9 ML in excellent agreement with our results for the first reactivity maximum. Earlier XPEEM studies by Aballe et al [18] report an enhanced total oxygen uptake for 7 ML which deviates slightly from theory and the chemicurrent results. The findings agree well with the nucleation and growth kinetics of the reaction as the first adiabatic charge transfer initiates the population of the diffusive precursor state. The chemicurrent measures the subsequent non-adiabatic electron transfers which happen when the diffusing charged molecule reaches the edge of an oxide island which we assume to be the active sites for oxygen dissociation.

5. Summary

Thin film Mg epilayers are fabricated on Si(111)-7 × 7 surfaces by low-temperature evaporation and soft annealing in the thickness range between 7 and 45 ML. The single-crystalline structure is demonstrated with LEED and UPS. In the photoelectron spectra characteristic QWSs are observed between the surface state at a binding energy of 1.6 eV and the Fermi level. Such disappear for polycrystalline and very thick metal overlayers. Chemicurrents are recorded in the thin-film Mg/p-Si(111) Schottky diodes upon exposure to molecular oxygen at a substrate temperature of 110 K. The current traces reveal a nucleation and growth mode of the magnesium oxide. The O_2 molecule is charged on the trajectory towards the surface in a first electron transfer (*harpooning*) into a mobile precursor state. It is eventually dissociated when it diffuses to an active surface site which is assumed to be at the edges of the growing oxide islands. The dissociation occurs non-adiabatically leading to e–h pairs in the metal film detected by the Schottky diode. For Mg epilayers of 9 and 13 ML the chemicurrent is more than doubled and the current trace is compressed on the exposure axis. This finding can be explained by an enhancement of the reaction rate by a factor between two and three. No device effects are involved as the oxygen uptake after large exposures measured with XPS is also enhanced for 9 and 13 ML Mg films. The QSE is interpreted by the electronic DOS at the Fermi level which is increased considerably when a QWS appears at E_F. The DOS is determined by measuring the photoelectron yield in normal direction which changes periodically with Mg film thickness. Whenever the DOS is large the oxidation rate is enhanced. Therefore, the first charge transfer which leads the molecule into the diffusive precursor state and which is mostly affected by the DOS decides on the total reactivity of the Mg epilayer surface. The experiments show in addition that the chemicurrent method is a very sensitive tool for live measurements of the surface reactivity of a system if at least one reaction step occurs non-adiabatically.

Acknowledgments

The financial support by the Deutsche Forschungsgemeinschaft (DFG-SFB616) is gratefully acknowledged.

References

[1] Ertl G, Knozinger H, Schüth F and Weitkamp J (ed) 2008 *Handbook of Heterogeneous Catalysis* 2nd edn (Hoboken: Wiley)
[2] Franke M E, Koplin T J and Simon U 2006 *Small* **2** 36
[3] Schweitzer P A 2009 *Fundamentals of Corrosion* (Boca Raton, FL: CRC Press)
[4] Anpo M (ed) 1995 *Surface Photochemistry* (Hoboken: Wiley)
[5] Hamann C H, Hamnett A and Vielstich W 2007 *Electrochemistry* (Hoboken: Wiley)
[6] Henry C R 1998 *Surf. Sci. Rep.* **31** 235
[7] Ertl G 2000 *Adv. Catal.* **45** 1
[8] Roldan Cuenya B, Baeck S-H, Jaramillo T F and McFarland E W 2003 *J. Am. Chem. Soc.* **125** 12928
[9] Haruta M 1997 *Catalysis Today* **36** 153
[10] Valden M, lai X and Goodman D W 1998 *Science* **281** 1647
[11] Choudhary T V and Goodman D W 2002 *Top. Catal.* **21** 25
[12] Heiz U and Landman U (ed) 2007 *Nanocatalysis* 2nd edn (Berlin: Springer)

[13] Nørskov J K, Bligaard T, Hvolbaek B, Abild-Pedersen F, Chorkendorff Ib and Christensen C H 2008 *Chem. Soc. Rev.* **37** 2163
[14] Hammer B and Nørskov J K 1995 *Surf. Sci.* **343** 211
[15] Lindberg V, Petersson T and Hellsing B 2006 *Surf. Sci.* **600** 6
[16] Li X-G, Zhang P and Chan C K 2007 *Physica* B **390** 225
[17] Ma X, Jiang P, Qi Y, Jia J, Yang Yu, Duan W, Li W-X, Bao X, Zhang S B and Xue Q-K 2007 *Proc. Natl Acad. Sci. USA* **104** 9204
[18] Aballe L, Barinov A, Locatelli A, Heun S and Kiskinova M 2004 *Phys. Rev. Lett.* **93** 196103
[19] Aballe L, Barinov A, Stojić N, Binggeli N, Mentes T O, Locatelli A and Kiskinova M 2010 *J. Phys.: Condens. Matter* **22** 015001
[20] Binggeli N and Altarelli M 2006 *Phys. Rev. Lett.* **96** 036805
Binggeli N and Altarelli M 2008 *Phys. Rev.* B **78** 035438
[21] Liu X, Wang C-Z, Hupalo M, Lin H-Q, Ho K-M and Tringides M C 2014 *Phys. Rev.* B **89** 041401(R)
[22] Lüth H 2010 *Solid Surfaces, Interfaces and Thin Films* 5th edn (Berlin: Springer) p 269
[23] Schulte F K 1976 *Surf. Sci.* **55** 427
[24] Feibelman P J 1983 *Phys. Rev.* B **27** 1991
[25] Hamawi A, Lindgren S-A and Walldén L 1991 *Phys. Scr.* **T39** 339
[26] Zhang Z, Niu Q and Shih C-K 1998 *Phys. Rev. Lett.* **80** 5381
[27] Chiang T-C 2000 *Surf. Sci. Rep.* **39** 181
[28] Aballe L, Rogero C and Horn K 2002 *Phys. Rev.* B **65** 125319
Aballe L, Rogero C and Horn K 2002 *Surf. Sci.* **518** 141
[29] Greber T 1997 *Surf. Sci. Rep.* **28** 3
[30] Glass S and Nienhaus H 2004 *Phys. Rev. Lett.* **93** 168302
Nienhaus H and Glass S 2006 *Surf. Sci.* **600** 4285
[31] Klar F, Bansmann J, Glaefeke H, Fitting H-J and Meiwes-Broer K-H 1999 *Surf. Sci.* **442** 477
[32] Gesell T F, Arakawa E T and Callcott T A 1970 *Surf. Sci.* **20** 174
[33] Nienhaus H 2002 *Surf. Sci. Rep.* **45** 3
[34] Nienhaus H, Bergh H S, Gergen B, Majumdar A, Weinberg W H and McFarland E W 1999 *Phys. Rev. Lett.* **82** 446
[35] Gergen B, Nienhaus H, Weinberg W H and McFarland E W 2001 *Science* **294** 2521
[36] Rhoderick E H and Williams R H 1988 *Metal-Semiconductor Contacts* 2nd edn (Oxford: Oxford University Press) p 90
[37] Nienhaus H, Krix D and Glass S 2007 *J. Vac. Sci. Technol.* A **25** 950
[38] Karlsson U Q, Hansson G V, Persson P E S and Flodström S A 1982 *Phys. Rev.* B **26** 1852
[39] Holloway P H and Hudson J B 1974 *Surf. Sci.* **43** 123
[40] Greber T 1998 *Appl. Phys.* A **67** 701
Greber T 1994 *Chem. Phys. Lett.* **222** 292